Supporting Information for

On the Friendship Paradox and Inversity: A Network Property with Applications to Privacy-sensitive Network Interventions

Vineet Kumar, David Krackhardt and Scott Feld

Corresponding Author: Vineet Kumar.
E-mail: vineet.kumar@yale.edu

This PDF file includes:

S.A. Local and Global Mean in Example Networks

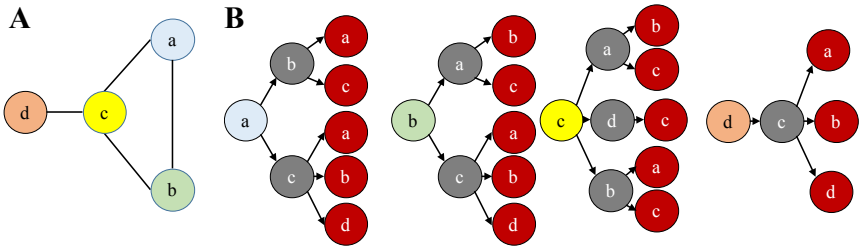

C Local Mean

a's local mean Friends of Friends: a has 2 friends (b and c); b has 2 friends and c has 3, so A's average number of friends of friends is $\frac{2+3}{2} = \frac{5}{2}$.

b's local mean Friends of Friends: Similar to a, it is $\frac{2+3}{2} = \frac{5}{2}$.

c's local mean Friends of Friends: c has 3 friends, $\frac{2+1+2}{3} = \frac{5}{3}$

d's local mean Friends of Friends: d has 1 friend $\frac{3}{1} = 3$

Average Number of Friends of Friends $= \frac{1}{N}\sum_i$[Node i's average number of friends of friends] $\mu_L = \frac{1}{4}\left(\frac{5}{2}+\frac{5}{2}+\frac{5}{3}+3\right) = \frac{29}{12}$

D Global Mean

We need to compute the **Total Number of Friends** and the **Total Number of Friends of Friends** in Network. a has 2 friends, b has 2, c has 3 and d has 1 friend. Thus, the total number of friends is (2+2+3+1) = 8.
For the **Total Number of Friends of Friends**, a has 5 friends of friends, b has 5, c has 5 and d has 3. So the total number of friends of friends = (5+5+5+3) = 18.

Average Number of Friends of Friends $= \frac{\text{Total Number of Friends of Friends}}{\text{Total Number of Friends}}$ $\mu_G = \frac{5+5+5+3}{8} = \frac{18}{8}$

Fig. S1. Local and Global Means in Example Network. **(A) Network.** Example network with 4 nodes a,b,c and d. **(B) Illustration of Friends and Friends of Friends.** Each node is mapped out with its friends and friends of friends. The node is in light blue, friends are in gray, and friends of friends are in red. Node a has 2 friends, b and c. Node a also has 5 friends of friends. **(C) Local Mean.** a has 2 friends, b and c. The total number of friends of friends in a's network is 5: (a's friend b has 2 friends, a and c; a's friend c has 3 friends, a, b and d). So, the average number of friends of friends for a is the ratio of the number of nodes in black to the number of nodes in red, i.e., $\frac{2+3}{2} = \frac{5}{2}$. Similarly, for the other nodes, we have $b: \frac{2+3}{2} = \frac{5}{2}$, $c: \frac{2+1+2}{3} = \frac{5}{3}$, $d: \frac{3}{1} = 3$. The local mean of the network is the mean of these local average friends of friends, so $\mu_L = \frac{1}{4}\left(\frac{5}{2} + \frac{5}{3} + \frac{1}{4} + \frac{3}{1}\right) = 2.42$. **(D) Global Mean.** Global mean is the ratio of the total number of friends of friends to the total number of friends. The total number of friends of friends contributed by a is 5. Similarly, b contributes 5, c contributes 5, and d contributes 3 friends of friends. Thus, the total number of friends of friends (i.e., the nodes in red) are $(5 + 5 + 5 + 3) = 18$. The total number of friends, represented by the nodes in gray, is $(2 + 2 + 3 + 1) = 8$.

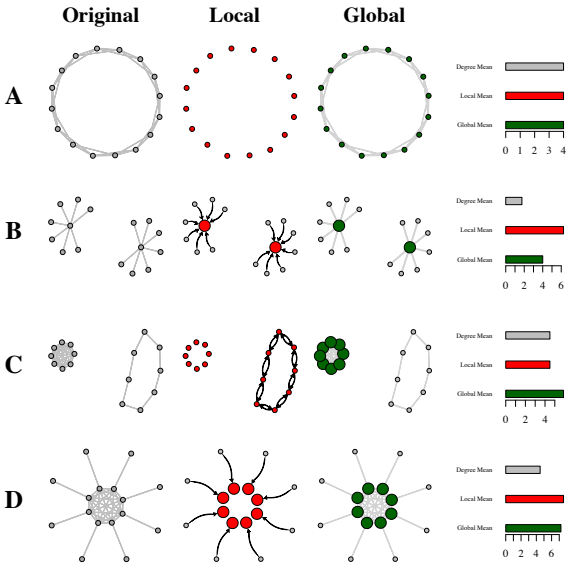

Fig. S2. Four Illustrative Networks with Varying Local and Global Means.
Each network in (A)-(D) has the original network plot (left), local weighted network (middle), and global weighted network (right). On the right is a barplot indicating the mean degree, local mean, and global mean for each of the networks. *Local Panel (Red)*: In the local weighted network plot (middle), nodes are sized proportional to their weight $\left(w_i^L\right)$ in contributing to the local mean. Edges that receive a *higher than median* weight in computing the local mean are in black. Otherwise, the edges are not plotted in the middle panel. Note that although the original networks are undirected, the selected edges are *directed*. *Global Panel (Green)*: Nodes are sized proportional to their weight $\left(w_i^G\right)$ in contributing to the global mean. Edges are all weighted equally in the global weighted network. (A) *Small World Ring:* Each node has four friends, and local and global mean are both equal to the average degree (4). None of the edges are shown in the middle panel since all edges have identical weight in computing the local mean. All nodes in both local and global means have the same weight and size in the middle and right panel. (B) *Two Central Hubs with Spokes:* Each central hub is connected to 7 nodes. The mean degree is lowest in this network. However, local mean is substantially higher than the global mean, and is higher than the mean degree across all networks (a)-(d). In the local panel, we see that the weight of central hubs has increased, whereas the corresponding weight for the low degree "spoke" nodes has decreased. In the global panel, the node weights are proportional to degree. (C) *Heavy Core with Detached Cycle:* The global mean is substantially higher than the local mean (and mean degree). Here, we see in the local panel that the weight of each of the nodes has not changed, and all nodes have the same weight. However, in the global panel, we see that the high degree nodes in the complete graph have higher weights compared to the original network, whereas the weights for the nodes in the 2-cycle are lower than in the original network. (D) *Heavy Core with Pendants:* Both the local and global mean are substantially higher than the mean degree. In the local panel, the edges connecting core nodes to other nodes (both core and pendant) have a relatively low weight, and are not displayed.

S.B. Mathematical Appendix

Formally, the network graph $\mathcal{G} = (V, E)$ is comprised of a set of N individual nodes and a set of undirected edges E. Each element of E is a pair of nodes, and (i, j) indicates an edge (connection) with $e_{ij} \in \{0, 1\}$. We also define the directed edge set $\hat{E}$ including both (i, j) and (j, i) as distinct elements of $\hat{E}$ corresponding to an undirected edge $i \leftrightarrow j$. Since the purpose is to conduct network interventions, we only consider nodes that are connected, and exclude isolates from the network. We detail the table of notation in Table S1.

Table S1. Table of Notation

Symbol	Term	Definition
$\mathcal{G}$,V,E	Network	Network Graph of Nodes V and Edges E
$\hat{E}$	Directed Edge Set	Each edge in E is replaced by two directed edges
D_i	Degree	Number of friends of i
$\mathcal{N}(i)$	Neighbors	*Set* of Friends of i
F_i	Average degree of friends of i	$\frac{1}{D_i}\sum_{j\in\mathcal{N}(i)} D_j$
μ_D, σ_D^2	Mean and variance of Degrees	$\frac{1}{N}\sum_i D_i$, $\frac{1}{N}\sum_i (D_i - \mu_D)^2$
μ_L	Local Mean	$\frac{1}{N}\sum_i F_i$
μ_G	Global Mean	$\frac{\sum_i D_i F_i}{\sum_i D_i}$
ρ	Inversity	$Corr\left(D_i, \frac{1}{D_j}\right) \forall (i,j) \in \hat{E}$

The basic idea of the friendship paradox can be expressed as "your friends have more friends than you." We examine the degree to which the friendship paradox holds for individual nodes, or the individual friendship paradox. We find in the result below that it cannot hold for all nodes, but can hold for an arbitrarily high proportion (< 1) of nodes.

Theorem S1. *For a finite network $\mathcal{G} = (V, E)$ and $\mathcal{N}_i$ is the set of i's connections. We find the following:*

(i) The friendship paradox statement, "on average, your friends have more friends than you do," specified as $\frac{1}{|\mathcal{N}(i)|}\left(\sum_{j\in\mathcal{N}_i} D_j\right) > D_i \ \forall i \in V$, cannot hold for all nodes in $\mathcal{G}$ or any connected component of $\mathcal{G}$.

(ii) There exists $\mathcal{G}$ for which the friendship paradox statement holds true for all nodes, except one.

Proof. Consider a multi-component network with C components, $V = \bigcup_{k=1}^{C} \mathcal{C}_k$, where each component $\mathcal{C}_k$ represents the set of nodes in a connected network.

To prove part (i) of the theorem, first consider each of the components in turn, with $k = 1$. First, in the trivial case of a degree-regular component, part (i) trivially holds. Next, consider the case with degree variation within component k. Within C_k, for a finite network, there must be a finite set of nodes $\mathcal{V}_k^{\max}$ with maximum degree within this component. At least one of the nodes in $\mathcal{V}_k^{\max}$ must then be connected to a node of lower degree; otherwise, the component would not be fully connected. Now, for that node, call it $i \in \mathcal{V}_k^{\max}$ connected to a node of lower degree, the friendship paradox statement $\frac{1}{|\mathcal{N}(i)|}\left(\sum_{j\in\mathcal{N}_i} D_j\right) > D_i \ \forall i \in \mathcal{C}_k$ cannot hold. Thus, for each component k, there is at least one node for which the friendship paradox statement does not hold. In the overall network $\mathcal{G}$, there must be at least C nodes for which the friendship paradox statement cannot hold.

For part (ii), we only need to consider the star or hub and spoke network. The friendship paradox statement can easily be verified to hold for all nodes except the central node. □

Theorem S2. *[Feld 1991] For a network $\mathcal{G} = (V, E)$ with degree mean μ_D and variance σ_D^2, the global mean of friends of friends is $\mu_G = \left(\mu_D + \frac{\sigma_D^2}{\mu_D}\right)$*

Proof. (as given in Feld, 1991). $\mu_G = \dfrac{\sum_i \sum_j e_{ij} D_j}{\sum_i D_i} = \dfrac{\sum_i D_i^2}{\sum_i D_i} = \dfrac{\mu_D^2 + \sigma_D^2}{\mu_D}$. We note that the above proof is not affected by isolates, since they add zero to both the numerator and denominator, leaving μ_G unchanged, whether or not we remove these isolates. □

Theorem S3. *For any general network $\mathcal{G} = (V, E)$ with mean degree μ_D, the local mean of friends is given by*

$$\mu_L = \mu_D + \frac{1}{2|V|} \sum_{(i,j)\in V\times V} e_{ij} \left[\frac{(D_i - D_j)^2}{D_i D_j}\right] \qquad [1]$$

where D_i is the degree of node i, and $e_{ij} \in \{0, 1\}$ indicates a connection between i and j.

Proof. Let D_i denote the number of connections of individual i, i.e., $D_i = \left| \{k \in V : \quad (i,k) \in E\} \right|$. Denote the set of neighbors of i by $\mathscr{N}(i) = \{k \in V : \quad (i,k) \in E\}$. Define $F_i = \frac{1}{D_i} \sum_{j \in N(i)} D_j$ as the mean number of friends for friends of i. The local mean is defined as:

$$\mu_L = \frac{1}{|V|} \sum_i F_i = \sum_{i \in V} \left[\frac{1}{D_i} \left(\sum_{j \in \mathscr{N}(i)} D_j \right) \right]$$

Rewriting the expression for μ_L in terms of the connections (edges) between individuals, we obtain:

$$\begin{aligned}
\mu_L &= \frac{1}{|V|} \sum_{i \in V} \left[\frac{1}{D_i} \left(\sum_{j \in V} e_{ij} D_j \right) \right] = \frac{1}{|V|} \sum_{i \in V} \sum_{j \in V} \left[e_{ij} \frac{1}{D_i} (D_j) \right] \\
&= \frac{1}{2|V|} \sum_{(i,j) \in V \times V} \left[e_{ij} \left(\frac{D_j}{D_i} \right) + e_{ji} \left(\frac{D_i}{D_j} \right) \right] = \frac{1}{2|V|} \sum_{(i,j) \in V \times V} e_{ij} \left[\frac{D_j}{D_i} + \frac{D_i}{D_j} \right] \\
&= \frac{1}{2|V|} \sum_{(i,j) \in V \times V} e_{ij} \left[\frac{D_j^2 + D_i^2}{D_i D_j} \right] = \frac{1}{2|V|} \sum_{(i,j) \in V \times V} e_{ij} \left[\frac{(D_i - D_j)^2 + 2 D_i D_j}{D_i D_j} \right] \\
&= \frac{1}{2|V|} \sum_{(i,j) \in V \times V} e_{ij} \left[\frac{(D_i - D_j)^2}{D_i D_j} \right] + \frac{1}{2|V|} (4|E|) \\
&= \mu_D + \frac{1}{2|V|} \sum_{(i,j) \in V \times V} e_{ij} \left[\frac{(D_i - D_j)^2}{D_i D_j} \right]
\end{aligned}$$

□

Note that what we characterize as the local mean defined above was independently shown to be greater than the mean degree, including by the present authors at (1). It has also been documented by others, including C. Borgs & J. Chayes in a comment to an article by (2), and by (3). However, the properties of the local mean have not been formally examined and characterized.

For the results below, we consider networks without isolates, even though the proofs hold in their presence.

Theorem S4. *Define the m-th moment of the degree distribution by $\kappa_m = \frac{1}{N} \sum_{i \in V} D_i^m$. The local and global means are connected by the following relationship involving the inversity ρ and the -1,1,2, and 3rd moments of the degree distribution:* $\mu_L = \mu_G + \rho \sqrt{\left(\frac{\kappa_1 \kappa_3 - \kappa_2^2}{\kappa_1} \right) \left[\kappa_{-1} - (\kappa_1)^{-1} \right]}$

Proof. We define the moments of the degree distribution as: $\kappa_m = \frac{1}{N} \sum_i D_i^m$. We defined inversity ρ as the correlation of two distributions that we specify as the origin degree (**O**) and inverse destination degree (**ID**) distributions. The **O** distribution consists of the degree of nodes corresponding to edges, and the **ID** distribution consists of the inverse degree of nodes corresponding to edges. Thus, each connection (edge) contributes *two* entries to *each* distribution. For example, if there is a connection between i and j, i.e., $e_{ij} = 1$, we would have $\left(D_i, \frac{1}{D_j} \right)$ and $\left(D_j, \frac{1}{D_i} \right)$. Observe that each individual appears in both distributions multiple times based on degree.

Next, we detail the mean and variance of the distributions. First, we consider the means. The mean of the origin distribution is $\mu_O = \frac{1}{2|E|} \sum_i D_i^2 = \frac{\mu_D^2 + \sigma_D^2}{\mu_D} = \mu_G = \frac{\kappa_2}{\kappa_1}$. Similarly, the **ID** mean is $\mu_{ID} = \frac{1}{2|E|} \sum_i D_i \left(\frac{1}{D_i} \right) = \frac{1}{\mu_D}$. Next, we consider the variances. The variance of the origin distribution (**O**) is computed as:

$$\begin{aligned}
\sigma_O^2 &= \frac{1}{2|E|} \sum_{(i,j) \in E} (D_i - \mu_O)^2 = \frac{1}{2|E|} \sum_{i \in V} D_i (D_i - \mu_O)^2 \\
&= \frac{1}{N \mu_D} \sum_{i \in V} \left[D_i^3 - 2 \mu_O D_i^2 + (\mu_O)^2 D_i \right] = \frac{\kappa_3}{\kappa_1} - \left(\frac{\kappa_2}{\kappa_1} \right)^2
\end{aligned}$$

Next, we express the corresponding variance of the inverse destination degree distribution (**ID**), σ_{ID}^2. Again, recall that $\frac{1}{D_i}$ does not appear just once, but D_i times. Therefore, we have:

$$\begin{aligned}
\sigma_{ID}^2 &= \frac{1}{2|E|} \sum_{(i,j) \in E} \left[\left(\frac{1}{D_j} - \frac{1}{\mu_D} \right)^2 \right] = \frac{1}{2|E|} \sum_{(i,j) \in E} \left(\frac{1}{D_j^2} + \frac{1}{\mu_D^2} - \frac{2}{\mu_D D_j} \right) \\
&= \frac{1}{2|E|} \left[\sum_{(i,j) \in E} \frac{1}{D_j^2} + \frac{1}{\mu_D^2} \left(\sum_{(i,j) \in E} 1 \right) - \frac{2}{\mu_D} \sum_{(i,j) \in E} \frac{1}{D_j} \right] = \frac{1}{2|E|} \left[\sum_{j \in V} \frac{1}{D_j} + \frac{1}{\mu_D^2} 2|E| - \frac{2}{\mu_D} N \right] \\
&= \frac{1}{\mu_D N} \left[\sum_{j \in V} \frac{1}{D_j} \right] - \frac{1}{\mu_D^2} \qquad = (\kappa_1)^{-1} \left[\kappa_{-1} - (\kappa_1)^{-1} \right]
\end{aligned}$$

We next turn to the inversity, and based on the definition, we connect it to the local and global means and the degree distribution.

$$\begin{aligned}
\rho &= \left(\frac{1}{2|E|\sigma_O\sigma_{ID}}\right)\sum_{(i,j)\in E} e_{ij}\left[(D_i-\mu_O)\left(\frac{1}{D_j}-\frac{1}{\mu_D}\right)\right] \\
(N\mu_D\sigma_O\sigma_{ID})\,\rho &= \left[\sum_{(i,j)\in E} e_{ij}\left(\frac{D_i}{D_j}\right)-\mu_O\left(\sum_{(i,j)\in E}\frac{1}{D_j}\right)-\frac{1}{\mu_D}\sum_{(i,j)\in E} D_i+\sum_{(i,j)\in E} e_{ij}\left(\frac{\mu_O}{\mu_D}\right)\right] \\
&= \left[N\left(\mu_L\right)-\mu_O\cdot N-\frac{1}{\mu_D}\sum_{(i,j)\in E} D_i+\sum_{(i,j)\in E} e_{ij}\left(\frac{\mu_O}{\mu_D}\right)\right] \\
&= \left[\left(N\mu_L\right)-N\mu_O-\frac{1}{\mu_D}\sum_{(i,j)\in E} D_i+2|E|\left(\frac{\mu_O}{\mu_D}\right)\right] \\
\implies \mu_L &= \mu_G+\rho\cdot\mu_D\cdot\ \sigma_O\sigma_{ID}
\end{aligned}$$

Finally, substituting $\mu_D=\kappa_1$ and the expressions for the variances, we obtain:

$$\mu_L=\mu_G+\rho\sqrt{\left(\frac{\kappa_1\kappa_3-\kappa_2^2}{\kappa_1}\right)\left[\kappa_{-1}-(\kappa_1)^{-1}\right]} \qquad [2]$$

□

Theorem S5. *The expected degree of nodes chosen by global strategy is the global mean.*

Proof. To determine the expected degree of a node chosen by the global strategy: Choose $M=1$ node initially, (say X). With probability q, choose each neighbor of X. For a node k with degree D_k, the probability of being chosen by this process is the first step when any of k's friends is chosen as the initial node, and the second step is k being chosen with probability q. This probability is $p_k=\frac{1}{N}\ D_k\times q=\frac{qD_k}{N}$. The expected degree of a chosen "seed" node is then the degree-weighted probability:

$$\frac{\sum_{k\in V}\ p_kD_k}{\sum_{k\in V}p_k}=\frac{\sum_{k\in V}\frac{1}{N}q\ D_k^2}{\sum_{k\in V}\frac{1}{N}q\ D_k}=\frac{\frac{1}{N}\sum_{k\in V}D_k^2}{\frac{1}{N}\sum_{k\in V}D_k}=\frac{\mu_D^2+\sigma_D^2}{\mu_D}=\mu_G$$

□

Similar logic applies if we choose any arbitrary initial sample of size M as long as the network is large, i.e., $N\gg M$.

Theorem S6. *[Rewiring Theorem] Let network $\mathcal{G}=(V,E)$ with $N>3$ nodes include nodes a,b,c,d with degrees ordered as: $D_a\le D_b<D_c\le D_d$. If there are nodes $a,b,c,d\in V$ such that $(a,b),(c,d)\in E$, but $(a,d),(b,c)\notin E$, then by rewiring the network to $\mathcal{G}'=(V,E')$, containing edges $(a,d),(b,c)\in E'$, but $(a,b),(c,d)\notin E'$, we obtain: $\mu_L(\mathcal{G}')>\mu_L(\mathcal{G})$ whereas $\mu_G(\mathcal{G}')=\mu_G(\mathcal{G})$. Also, it follows that $\rho(\mathcal{G}')>\rho(\mathcal{G})$.*

Proof. First, observe that the degree distribution is unaffected by the change, since each node's degree is unchanged by the rewiring. Therefore, the global mean (which only depends on mean and variance of the degree distribution) is also unaffected, i.e., $\mu_G(\mathcal{G})=\mu_G(\mathcal{G}')$. Recall that the local mean is $\mu^L=\frac{1}{N}\sum_i\sum_j e_{ij}\left[\frac{D_i}{D_j}+\frac{D_j}{D_i}\right]$. Since between $\mathcal{G}$ and $\mathcal{G}'$ the degrees of all nodes are the same, and all edges are the same except the two rewired edges, we can write the difference between their local means as:

$$\begin{aligned}
\mu^L(\mathcal{G}')-\mu^L(\mathcal{G}) &= \frac{1}{N}\left[\left(\frac{D_a}{D_d}+\frac{D_d}{D_a}+\frac{D_b}{D_c}+\frac{D_c}{D_b}\right)-\left(\frac{D_a}{D_b}+\frac{D_b}{D_a}+\frac{D_c}{D_d}+\frac{D_d}{D_c}\right)\right] \\
&= \frac{1}{N}\left[(D_d-D_b)\left(\frac{1}{D_a}-\frac{1}{D_c}\right)+(D_c-D_a)\left(\frac{1}{D_b}-\frac{1}{D_d}\right)\right]>0
\end{aligned}$$

The last inequality follows from the ordering of the node degrees. Note that we actually only require the conditions $D_b<D_d$ and $D_a<D_c$ to hold. Since the degree distribution does not change with rewiring, by Theorem S4, we must have an increase in inversity, $\rho(\mathcal{G}')>\rho(\mathcal{G})$.

□

S.C. Data on Real Networks

We use a wide variety of real networks to characterize their properties, and illustrate how relate to the interventions detailed in the paper. We use data from two repositories.

A. Koblenz Network Collection. The networks are selected across several categories (Affiliation, Face-to-face Social, Online Social, Computer, Infrastructure and Biological networks), and span a wide range in network characteristics like size and density (Table S2). These networks also vary widely in terms of their size, from a low of 25 to networks with millions of nodes (e.g., Youtube). All network data was obtained from the Koblenz Network Collection (KONECT) (4). We examine these real networks on a number of dimensions, including the number of nodes, edges, and the variation in the degree distribution.

Table S2. Real Network Characteristics

Label	Network	N	$\|E\|$	μ_D	μ_L	μ_G	ρ
Collaboration							
A1	Actor-Movie	383640	1470338	7.67	36.29	35.12	0.02
A2	Club Mmebers	25	91	7.20	10.39	9.39	0.39
A3	Citation (Physics)	28045	3148413	224.53	569.15	667.24	-0.06
A4	Citation (CS)	317080	1049865	6.62	18.53	21.75	-0.10
Face-to-Face Interaction							
FS1	Physician	117	464	7.93	10.19	9.95	0.09
FS2	Adolescent Health	2539	10454	8.23	9.85	10.49	-0.20
FS3	Contact	274	2124	15.50	74.78	56.69	0.26
FS4	Conference	410	2765	13.49	17.10	18.72	-0.19
Online Social							
OS1	PGP Users	10679	24315	4.55	13.46	18.88	-0.17
OS2	Flickr	105722	2316667	43.83	187.12	349.21	-0.22
OS3	Advogato	5042	40509	15.56	99.31	82.52	0.06
OS4	Twitter	465016	833539	3.58	437.74	226.53	0.65
Topology of Computer Networks							
C1	Internet Topology	34761	107719	6.20	530.34	319.46	0.22
C2	WWW (Google)	855802	4291352	10.03	226.59	170.35	0.06
C3	Gnutella P2P	62561	147877	4.73	13.22	11.60	0.15
Infrastructure							
I1	Power Grid	4941	6593	2.67	3.97	3.87	0.06
I2	US Airports	1572	17214	21.90	120.27	112.23	0.04
I3	CA Roads	1957027	2760387	2.82	3.15	3.17	-0.04
Biological							
B1	Human Protein 1	2783	6222	4.32	19.61	15.78	0.15
B2	Human Protein 2	5973	146385	48.81	117.83	143.31	-0.09
B3	Yeast Protein	1458	1970	2.67	9.65	7.13	0.31
B4	C. Elegans	453	2033	8.94	51.57	40.10	0.21

A few observations are worth noting here. First, there are many networks with both positive and negative values of inversity, both within and across categories. Second, we do not see Inversity close to ± 1. However, the Twitter network is closest in magnitude, with an inversity of 0.65. Third, the variation in inversity is low in some categories like Infrastructure, whereas it is relatively greater in Online Social networks. Finally, we see that even low values of inversity can impact the difference between the local and global mean significantly, as well as between these and the mean degree. The WWW (Google) network, for example, displays such meaningful differences, even with a low inversity value of 0.06. This is due to the multiplier effect of the moments of the distribution function, detailed in equation (3).

B. India Village Networks. In addition, we also use data from $N = 75$ villages in India made publicly available (see (5) for details). The summary statistics for those village household networks are detailed in Table S3.

Table S3. Summary Statistics of Village Networks

Network Statistic	Mean	SD	Min	Max
Number of households	216.69	61.22	77	356
Number of (undirected) edges	993.31	348.77	334	2015
Density	0.05	0.02	0.02	0.11
Degree Mean	9.10	1.573	6.13	12.78
Degree Variance	52.03	19.88	27.80	124.56

S.D. Individual Friendship Paradox

A basic view of the friendship paradox is developed by plotting the average number of friends (degree) of individual nodes' "friends" on the vertical axis against the average degree (Fig. S3, Fig. S4). For example, in the Contact (In-person Social) network, we see a deep blue region above and to the left of the 45° line. Although present across all networks, the pattern is most prominent in the WWW (Google) or Twitter (Online Social) network. Observe also that in the Road Network, only $\Delta = 37\%$ of nodes have a higher average number of friends of friends than their own degree.

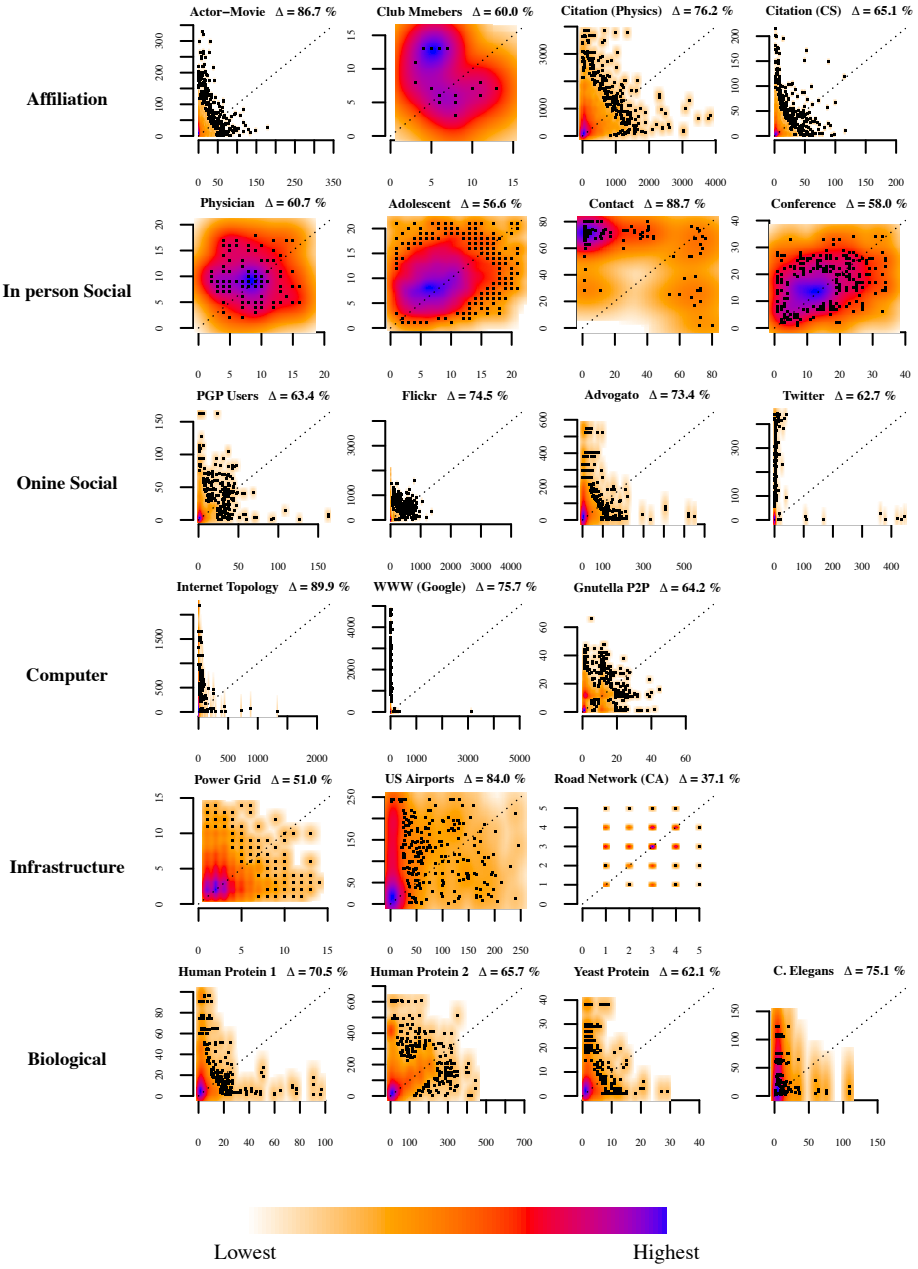

Fig. S3. Friendship Paradox at Individual Level. Density plot of average number of friends of nodes compared to node degree in networks. Δ indicates the proportion of nodes that have a higher average number of friends of friends than their degree. Lowest density regions within each network are marked by white / orange, and highest density regions are marked in blue. For all networks, the highest density region lies above and to the left of the 45 degree line. For some networks like Adolescent Health or Road Network (CA), it is relatively more evenly distributed both above and below the 45 degree line, whereas for networks like Internet Topology or Twitter, the distribution is skewed above and to the left.

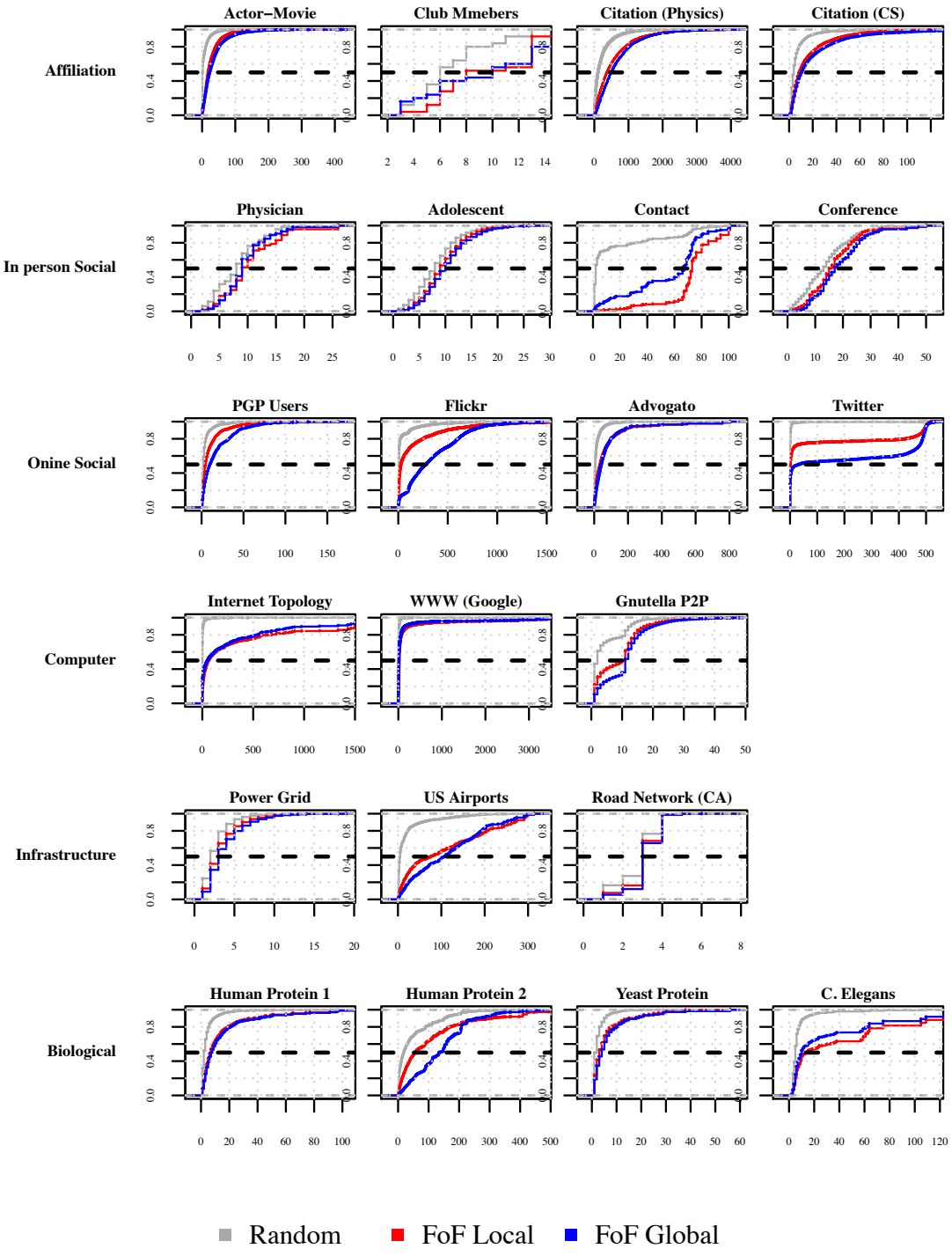

Fig. S4. Individual Friendship Paradox. Empirical Cumulative Distribution Functions (CDF) of Real Networks. Panels show the CDF of 3 different network properties at the individual node level. For a specific node degree, the probability that a node with a lower (or identical) degree is chosen by the sampling strategy for Node Degree (gray), Local Mean of Friends of Friends (FoF Local in red), and Global Mean of Friends of Friends (FoF Global in blue). Across all networks, for lower degrees, the Node Degree curve is to the left of the Local and Global Mean of Friends curves. In several networks, Global Mean of Friends is to the left and higher than Local Mean of Friends (e.g., Contact), whereas in others, it is to the right (e.g., Flickr).

We illustrate this "individual friendship paradox" using a scatterplot of the node degree versus the average friend degree in Figure S4. Nodes that have a higher degree than their average friends are colored red, whereas nodes that have lower degrees are colored blue. Across most real networks, we observe that the nodes in blue vastly outnumber the nodes in red. Relatedly, there are several nodes with low degrees, whose friends on average have a high degree.

S.E. Leverage in Generated Networks

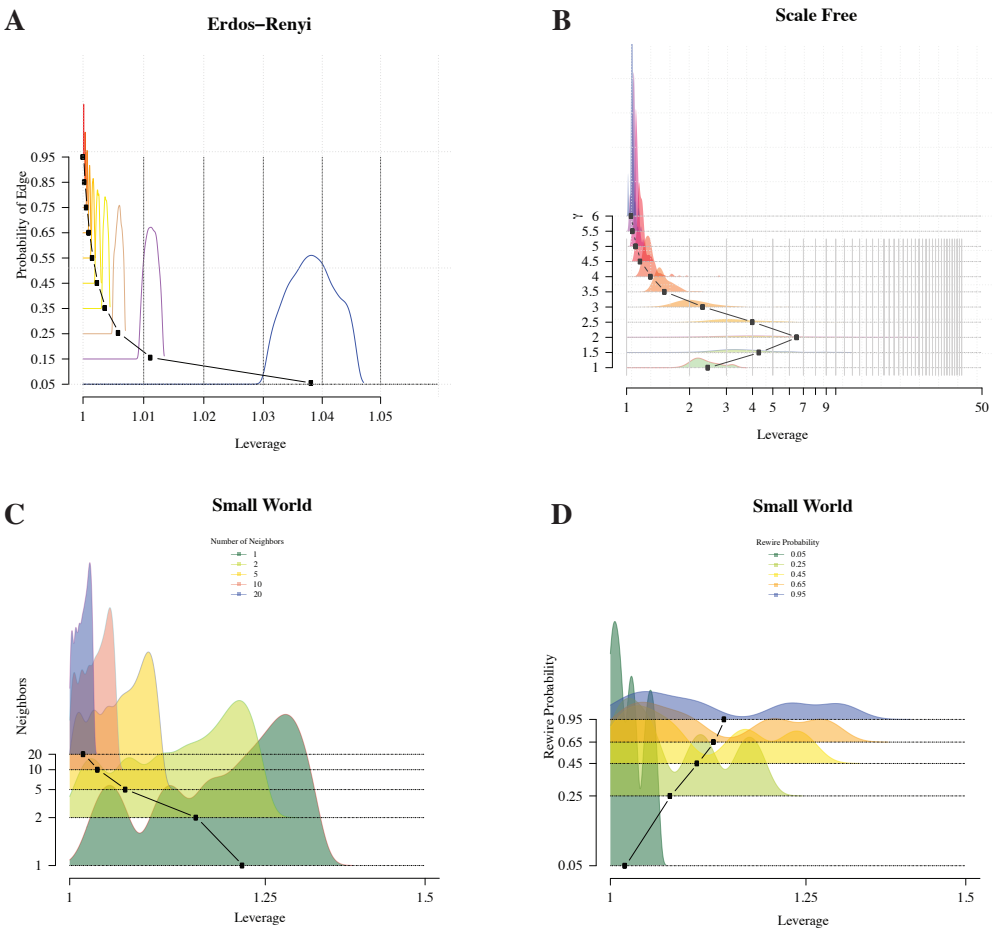

Fig. S5. Local Leverage Density in Generated Networks from three different generative models, spanning the parameter space of each. A sample of 1,000 networks was used for each of the models. (A) Erdos-Renyi (ER) networks generated with edge probabilities, $p \in [0.05, 0.95]$, and size ranging from N=50 to N=1,000 nodes. We find that local leverage is highest for the lowest edge probabilities, and leverage converges to 1 as the networks become more dense. (B) (SF) Static Scale Free networks with scale-free parameter $\gamma \in [1, 6]$ (6). For these networks, observe that the leverage spans a wider range, e.g., for $\gamma = 2$, the samples range from leverage of 1 to over 40. The mean leverage is non-monotonic in terms of γ, increasing when $\gamma < 2$ and decreasing for $\gamma > 2$. The distribution of leverage across the samples also displays decreasing variance when $\gamma > 2$. At very high levels of $\gamma \approx 6$, the local mean converges to the mean degree. With (SW) small world networks, we have two parameters (7). First is the number of neighbors each node is connected to initially, n. The edges are then rewired with a specified probability, p_r. First, in panel (C), we find that with a small number of neighbors, the leverage distribution is quite spread out, and there is a substantial leverage effect. However, as we begin to create very dense networks, both the mean and the variance of the leverage distribution diminish substantially. Second, we examine the impact of rewiring probability on the leverage distribution in panel (D). We find that with lower rewiring probabilities, say $p_r = 0.05$, the leverage distribution is closer to 1, whereas with higher rewiring probabilities, the distributions feature increased variance as well as higher mean leverage.

S.F. Network Features that Impact Inversity

Inversity is strongly dependent on the structure of connections, who is connected to whom. We observe in the main paper that star-type network structures lead to positive values of inversity, whereas clusters or cliques contribute to negative inversity values.

Star or hub-based networks First, we observe that there is significant evidence for hub-based network structures appearing in real-world networks. Such hub-like structures are common across a wide range of networks, including co-author networks, the underlying interlink network that forms the Internet, as well as Airline networks (8–11). The early networks literature explaining the emergence of such hub-like patterns posited preferential attachment as a mechanism, where newly joining nodes connected disproportionately to highly connected nodes (6, 12). The economics literature involving the economic incentives underlying network formation posits that agents form links based on the expected benefits to such formation. The resulting network is an equilibrium outcome based on the decisions of each of the agents, who are maximizing their own utilities (13). In this stream, an influential paper (14) finds that even when agents are homogeneous — where they have identical constraints, preferences, and incentives — *star networks arise across a wide range of equilibria*. Stars are predicted to occur even though agents are symmetric with identical incentives and opportunities. Complementing this research, star networks are found to arise over time in experimental settings where agents vary in terms of costs, incentives, and even information (15).

Clusters and Communities in networks Clusters or communities as well as cliques (fully connected or complete subnetworks) are commonly observed in networks. A typical conceptualization of community is the following: "Qualitatively, a community is defined as a subset of nodes within the graph such that connections between the nodes are denser than connections with the rest of the network." (16). There are several reasons why communities form, including homophily and social foci. In homophily, when a number of individuals are similar, then they are much more likely to be connected to each other, and also part of the same larger grouping or community (17). However, it should be noted that not all such connections will happen; rather, such connections and communities are more likely to happen when individuals are homophilous. We note that homophily has also been tied to polarization and segregation (18).

A prominent theory that explains how communities form is the idea of foci (19). The essential idea is that most ties originate around foci of activity, where a limited set of people share a focus that organizes activity, and thereby tend to generate repeated interaction among the same people in the set over time that leads to ties among many of them. Each person tends to be associated with many different foci. Alters from the same focus tend to be tied to one another, but not those from separate foci. Consistent with this notion, research has found that the way organizational environments are structured moderates the tie-formation process (20).

An implication of this theory for the present paper is that larger, denser foci of activity contribute large numbers of ties for all their tied participants, and small and/or sparse focused sets generate few for their participants. Thus, the size and density of focused sets may contribute to positive or negative inversity.

S.G. Inversity and Assortativity: Connections and Differences

A natural question is whether inversity, $\rho = Corr\left(D^{\mathbf{O}}, \frac{1}{D^{\mathbf{D}}}\right)$, captures the same information (with opposite sign) as degree assortativity, which is a well known network property, $\rho_a = Corr\left(D^{\mathbf{O}}, D^{\mathbf{D}}\right)$.(21–23). Inversity and assortativity are negatively correlated, as we might expect.

Can Assortativity Be Used as a Proxy for Inversity?. There are several specific reasons why we don't think it is a good idea to use assortativity as a *proxy metric* in place of inversity. We demonstrate specifically how using assortativity as a proxy for inversity would lead to incorrect choices to the network intervention questions below.

Network Intervention Questions: We begin with our objective for the network intervention strategies, which is to choose a strategy that maximizes the expected degree of target nodes. We have two questions that need to be answered.

(A) Identify whether the local strategy leads to higher expected degree than the global strategy (or vice versa), i.e. whether $\mu_L > \mu_G$ or $\mu_G > \mu_L$.

(B) Evaluate the improvement in expected degree offered between any of random, local and global strategies, i.e. $(\mu_L - \mu_D)$, $(\mu_G - \mu_D)$ and $(\mu_L - \mu_G)$.

The requirements for problem (A) are different from those of (B). For (A), we need to just know the correct ordering of local and global strategies, and not the magnitude. Inversity (ρ) gives us a direct answer to question (A), since $\mu_L > \mu_G \iff \rho > 0$. For (B), the ordering is not sufficient, and we need to know the magnitude, and we explore this below.

Why Magnitudes of Differences Matter: The decision maker could evaluate the benefit of using a friendship paradox strategy is worth the potential cost relative to the random strategy, which requires the least amount of information and effort from the people originally selected. Thus, the decision maker would trade off the increase in expected degree relative to the marginal cost of using the strategy (24). This logic implies that knowing just the ordering of the different strategies is not sufficient, and *we would need to know the magnitudes of the differences* in order to select a strategy.

Inversity allows for a direct linear transformation from global mean (μ_G) to local mean (μ_L) calculation of friends of friends. We can see this using the formulation from equation (2) in page 5 of this Supplement:

$$\mu_L = \mu_G + \rho \underbrace{\left(\sqrt{\left(\frac{\kappa_1\kappa_3 - \kappa_2^2}{\kappa_1}\right)\left[\kappa_{-1} - (\kappa_1)^{-1}\right]}\right)}_{\omega} = \mu_G + \rho\ \omega$$

where the κs represent the moments of the degree distribution. This formula implies that $\mu_L = \mu_G + \omega\rho \implies \mu_L - \mu_G = \omega\rho$, where ω is a function of the moments of the degree distribution.

We have found no comparable transformation between global and local means using assortativity, and argue that such a relationship is unlikely to exist (see point below about monotonic ordering between these metrics). Thus, to use assortativity in place of inversity, we must first assume $\rho_a \approx -\rho$ in order to make an approximation of the form: $\mu_L - \mu_G \approx -\omega\rho_a$. We don't know whether and when this approximation would be valid.*

If we do make this approximation, high values of the quantity ω can amplify small differences in the values of ρ. Therefore, even *small errors* in approximating inversity with assortativity would be highly problematic in evaluating magnitude of effect sizes. We also see that this impact is practically important. In Table S2 of Supplement §S.C, for instance, we observe that even small values of inversity can result in large differences between the different means. Please see the statistics corresponding to the A3 (Citation) and C2 (WWW) networks.

Decisions using Assortativity versus Inversity: Inversity is sensitive to and positively affected by stars and star-like structures. Assortativity, on the other hand, is more sensitive to and positively affected by cliques and clique-like structures. Supplement §S.F shows that cliques and stars are commonly present in real world networks.

Illustative Example Networks by Simulation: We explore this logic quantitatively by simulating specific type of networks with stars and cliques to make things concrete. Characterizing all the networks where such results would occur is an interesting question for future research, but beyond the scope of the present paper.

We fix the number of cliques to 100 and allow clique sizes in the range from 2 to 100 nodes (random with uniform probability). We add only one star network and vary the size of the star network, with the number of nodes in the star varying from 1 to 1500. We plot in Figure S6 both the assortativity and inversity levels for each network as a function of how large the star is in the network. All other parameters remain fixed. The blue circles indicate the inversity (ρ) for the generated network; the red plus-signs indicate the assortativity (ρ_a) for the same generated network.

First, we note that inversity and assortativity are highly correlated. However, if we use assortativity as a proxy for inversity, we would not make the right decisions for (A) or (B). Using assortativity as proxy, we would approximate $\rho \approx -\rho_a$. We now detail the problems with using assortativity:

*We further note that without Theorem S5, it would not be possible to quantify the differences between local and global means in terms of the degree distribution and inversity.

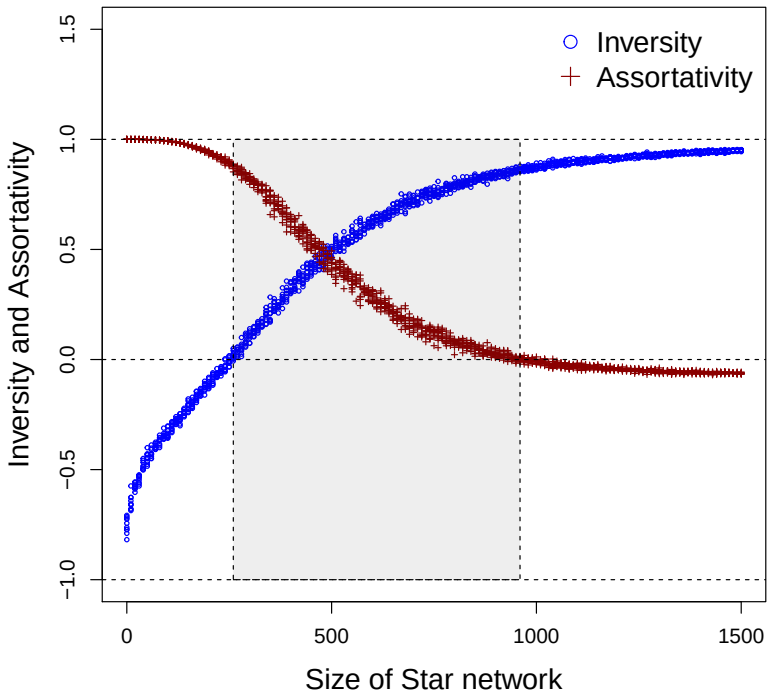

Fig. S6. How Inversity and Assortativity Vary with Size of Star Network

Note: We simulate networks with one star and 100 cliques. The size of the cliques varies randomly (uniform distribution) between 2 and 20 nodes. The size of the star network is varied between 1 and 1500 (one hub connected to 1500 spokes). We do $n_s = 10$ simulations for each size of the star network, and each network appears in the plot as a point. We observe that inversity is increasing with size of the star network, whereas assortativity is decreasing. The shaded area represents a region among these simulated graphs where *both inversity and assortativity are positive*.

(1) In the shaded region, where the size of the star networks is between 260 and 960 (approximately), we observe that the sign of assortativity and inversity is the same, i.e., *both are positive*. In such a case, the answers to both questions (A) and (B) would be incorrect.

(2) To the left of the shaded region, where the size of the star network varies from 1 to 260 (approximately), we note that $|\rho_a| > |\rho|$, implying that even though the sign of ρ_a and ρ are opposite, the magnitudes are quite different. More specifically, assuming $\rho \approx -\rho_a$, we would overestimate the benefit of the local strategy, leading to errors in answering question (B).

(3) To the right of the shaded region, i.e., when star networks have size greater than 960, we observe that $|\rho| \gg |\rho_a|$, specifically $|\rho| \approx 1$, whereas $|\rho_a| < 0.1$. This difference in magnitudes implies that using the proxy assumption $\rho \approx -\rho_a$ would be highly problematic for obtaining magnitudes required for (B). More specifically, we would substantially underestimate the benefits of the local strategy relative to global and random.

Broadly, in these networks, assortativity cannot reliably help us determine which mean (local or global) is larger, or which strategy dominates. We also don't know the conditions under which it could serve (or not) as a reasonable proxy for inversity for these or more general networks. Thus, even when these metrics are highly correlated, using the proxy of assortativity in place of inversity could lead to errors over a substantial range of networks.

Monotonic Ordering between Assortativity and Inversity? Since Assortativity (ρ_a) as a proxy is directionally the *reverse* of Inversity (ρ), we would naturally expect that it to vary monotonically with inversity. Specifically, we would expect for any pair of networks $\mathcal{G}_1$ and $\mathcal{G}_2$, when $\rho(\mathcal{G}_1) > \rho(\mathcal{G}_2) \iff \rho_a(\mathcal{G}_1) < \rho_a(\mathcal{G}_2)$. However, there are (many) examples of pairs of networks where both assortativity are directionally the same, i.e. $\rho(\mathcal{G}_1) > \rho(\mathcal{G}_2)$ and $\rho_a(\mathcal{G}_1) > \rho_a(\mathcal{G}_2)$. Using common network generation algorithms, it is easy to obtain many such pairs of networks, where one of the networks has both **higher assortativity *and* higher inversity** than the other. Thus, we find that assortativity as a proxy metric for inversity does not even preserve ordering, making it problematic to rely on it as a proxy for network intervention problems.

S.H. Virus Propagation Models

We detail below several examples of virus propagation models being used for characterizing the transmission and spread of diseases. These models build upon the early work of Kermack and McKendrick (25). All individuals in a population (in our case, the nodes in a network) are in one of the states, either susceptible (S) or infected (I). Based on the viral propagation, they can move to other states like Exposed (X), Recovered (R), or Deceased (D). For example, the SIR model involves individuals being in one of three states, (S), (I) or (R), and transitioning between the states probabilistically. Typically, the vast majority of nodes are present in the susceptible state (S), in which they might contrast the disease. The exposed state (X) is used to indicate a node that has been exposed to the disease, but could be asymptomatic during an incubation period and is not capable of infecting others. In contrast, the infected state (I) indicates a node that is capable of infecting others. The (R) recovered state implies permanent immunity. There are further extensions possible, e.g., adding infants who have maternal antibodies (state M) that provide passive immunity. See (26) or (27) for an overview and survey of these models. These models have been extensively used in epidemiological studies to characterize disease dynamics as detailed in Table S4, including measles, influenza, and COVID-19.

There has been recent notable work that aims to characterize the epidemic thresholds of these compartmental models with disease transmission over a network (28, 29). The critical idea is that the epidemic threshold of a network can be characterized as the inverse of the greatest (first) eigenvalue of the adjacency matrix A of the network, denoted as:

$$\boxed{\tau(A) = \frac{1}{\lambda_1(E)}}$$

.

Eigenvalue λ_1, termed the spectral radius, characterizes the connectivity of the network graph. Thus, networks that have higher connectivity or λ_1 are more likely to allow contagions along different paths to grow into epidemics, whereas in networks with low connectivity, contagions are more likely to die out.

While there have been a number of epidemic thresholds for specific network generating processes (e.g., small world), the generality of the result above is valuable since it allows: (a) any arbitrary network, without placing restrictions on its topology or structure, and (b) a wide range of compartmental models like SIS, SIR, and others detailed in Table S4 typically used to model infectious disease.

Whereas we consider an SIR model for illustration, the results also hold for the other models. The model is parametrized by two rates: β is the probability of an infected node infecting a susceptible node in a given time period, and δ is the probability at which an infected node recovers (or is cured) during the period. If time is continuous, β and δ can be viewed as the rates of infection and recovery. In either case, $\mathcal{R}_0$ is defined as $\boxed{\mathcal{R}_0 = \frac{\beta}{\delta}}$.

The epidemic threshold τ is defined as follows (28):

$$\boxed{\begin{cases} \mathcal{R}_0 = \dfrac{\beta}{\delta} < \tau(E) \implies \text{infection dies out over time} \\ \mathcal{R}_0 = \dfrac{\beta}{\delta} > \tau(E) \implies \text{infection grows over time} \end{cases}}$$

There are a few observations relevant here. First, the critical value of epidemic threshold is a function of the adjacency matrix E of the network topology (structure) $\mathcal{G}$. Second, a network topology with a higher epidemic threshold is less likely to have an epidemic. Third, interventions like immunizing nodes or reducing the number of connections (edges) can increase the threshold $\tau(E)$ so that infections are more likely to die out.

Table S4. Virus Propagation Models Used for Diseases

Virus Propagation Model	Infectious Diseases [References]
SIS	Malaria ((30))
SIR	Measles (31), Swine Flu H1N1 (32), Ebola (33)
SXIR	Chicken Pox (34), SARS (35), COVID-19 (36)
SIRD	COVID-19 ((37))

Note: The states refer to (**S**)usceptible, (**I**)nfectious, (**R**)ecovered / (**R**)emoved, (**X**)Exposed, (**D**)eceased

Implementation of VPM. We begin with a seed set of 1% of the nodes being infected, and evaluate epidemic outcomes using the SIR model. All the nodes in the network that are not infected or recovered are susceptible (S) to the infection. Each infected node can transmit an infection in each period probabilistically to each of its neighbors. The probability of an infection is

$P_{\text{transmit}} = \beta$. Thus, a node can become infected (I) from contact with any of its neighbors. In each period, an infected node can be cured or recovered (R) probabilistically, with the likelihood $P_{\text{cure}} = \delta$. Recovered nodes cannot be reinfected and cannot transmit infections.

The process of immunizing (or vaccinating) a set of nodes involves choosing a proportion of nodes (5%, or 10% or 20%) and ensuring that these nodes do not transmit any disease. The nodes for immunization are chosen based on three strategies: random, local, and global. The parameters used in the simulation of the epidemic are detailed in Table S5.

Table S5. Parameters of SIR Network Propagation Model

Parameter	Value	Description
$P_{\text{transmit}} = \beta$	0.20	Probability of an infected node transmitting the disease to a susceptible neighbor.
$P_{\text{cure}} = \delta$	0.15	Probability of an infected node recovering. Thus, moving from (I) $\implies$ (R) is $P_{I \to R} = P_{\text{cure}}$, and $P_{I \to I} = 1 - P_{\text{cure}}$
$P^k_{S \to I}$	$1 - (1 - \beta)^{N^{\text{infected}}_k}$	Probability of a susceptible node k becoming infected. Depends on the number of infected neighbors N^{infected}_k. Thus, k can become infected through *any* of its infected neighbors. So we have: $P^k_{S \to I} = 1 - (1 - P_{\text{transmit}})^{N^{\text{infected}}_k}$. Similarly, $P^k_{S \to S} = (1 - P_{\text{transmit}})^{N^{\text{infected}}_k}$.
n^0_{infected}	1%	Proportion of nodes in network that are infected at the beginning
n_{sim}	100	Number of simulations

Note: (**S**)usceptible, (**I**)nfectious, (**R**)ecovered / (**R**)emoved

Thus, a strategy A is better than an alternative strategy B if it results in lower levels of peak infections, total infections, and total suffering.

S.I. Epidemic Outcomes

In Figure S7, we examine the epidemic propagation characteristics on the Facebook network (38) using the same parameters as detailed in Table S5. The epidemic could be viewed as an *informational* epidemic propagating through Facebook. Alternatively, one might consider the Facebook network structure to serve as an approximation of contact network for the purposes of this evaluation.

We evaluate epidemics using the following metrics:

- **Proportion Infected at Peak** $= \frac{1}{N} \max_t(\sum_i I_{it})$: Since epidemics increase in intensity and eventually die down, an important characteristic is to measure the proportion of the population who are infected at the peak of the epidemic. This directly impacts important decisions like hospital capacity planning, etc.
- **Proportion Ever Infected** $= \frac{1}{N} \sum_i \max_t(I_{it})$: The proportion of the population that was ever infected by the disease is important since it represents the total spread of the disease in the population. It could also represent the number of people who might have immunity to future recurrences of the disease.
- **Total Suffering**: $\frac{1}{NT} \sum_i \sum_t (I_{it})$ Here, the total suffering metric captures not just how many infections occur, but also the length of the infections. This represents the proportion of individual-period combinations with an infection.

For the Facebook network sample, we find that an epidemic's outcomes are better when using the local strategy compared to the global strategy, which in turn is better than the random strategy. This conclusion holds for all the metrics considered above.

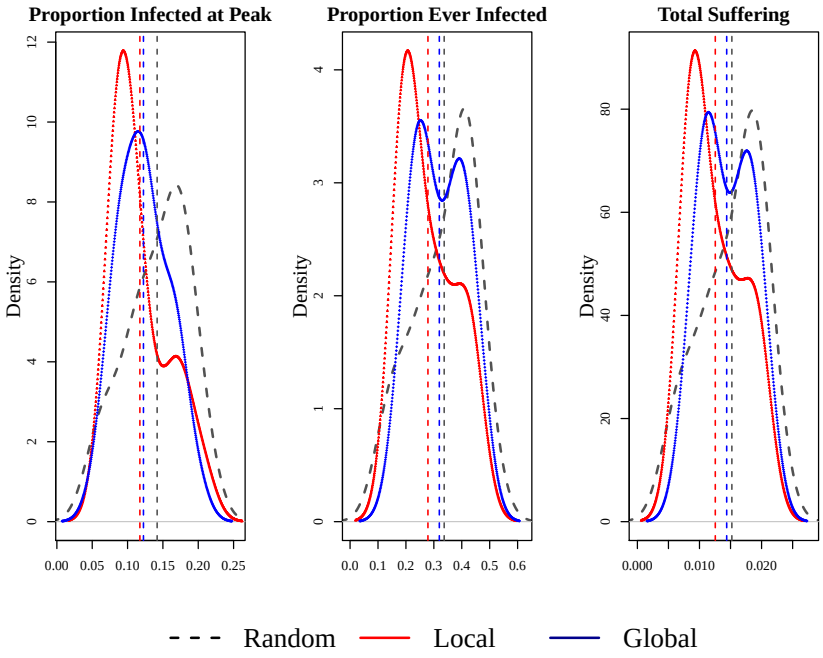

Fig. S7. Epidemic Outcomes with Immunization in Facebook Network. See Table S5 for parameters of simulation. All outcomes are density plots. We plot 3 outcomes: (a) the proportion of population infected at the peak, (b) proportion of population that was ever infected, and (c) total suffering. In each panel, the x-axis represents proportions and the y-axis represents density. We plot the outcomes for 3 strategies: (R)andom, (L)ocal, and (G)lobal. The dashed vertical lines represent the means for the 3 strategies. We find that for the Facebook network, the Local strategy is better for all outcomes than the Global, which in turn is better than the Random strategy.

References

1. V Kumar, D Krackhardt, S Feld, Why your friends are more popular than you are - a revisit in *Archives of the 33rd Sunbelt Conference of International Network for Social Network Analysis*. (INSNA), (2013).
2. S Strogatz, Friends you can count on. *The New York Times* **September 17** (2012).
3. MO Jackson, The friendship paradox and systematic biases in perceptions and social norms. *J. Polit. Econ.* **127**, 777–818 (2019).
4. J Kunegis, Konect: the Koblenz network collection in *Proceedings of the 22nd International Conference on World Wide Web*. (ACM), pp. 1343–1350 (2013).
5. A Banerjee, AG Chandrasekhar, E Duflo, MO Jackson, The diffusion of microfinance. *Science* **341**, 1236498 (2013).
6. AL Barabási, R Albert, Emergence of scaling in random networks. *Science* **286**, 509–512 (1999).
7. D Watts, S Strogatz, Collective dynamics of "small-world" networks. *nature* **393**, 440–442 (1998).
8. AL Barabâsi, et al., Evolution of the social network of scientific collaborations. *Phys. A: Stat. mechanics its applications* **311**, 590–614 (2002).
9. ME Newman, Coauthorship networks and patterns of scientific collaboration. *Proc. national academy sciences* **101**, 5200–5205 (2004).
10. S Goyal, MJ Van Der Leij, JL Moraga-González, Economics: An emerging small world. *J. political economy* **114**, 403–412 (2006).
11. ME O'Kelly, HJ Miller, The hub network design problem: a review and synthesis. *J. Transp. Geogr.* **2**, 31–40 (1994).
12. AL Barabási, , et al., Scale-free networks: a decade and beyond. *science* **325**, 412 (2009).
13. MO Jackson, , et al., *Social and economic networks*. (Princeton university press Princeton) Vol. 3, (2008).
14. V Bala, S Goyal, A noncooperative model of network formation. *Econometrica* **68**, 1181–1229 (2000).
15. JK Goeree, A Riedl, A Ule, In search of stars: Network formation among heterogeneous agents. *Games Econ. Behav.* **67**, 445–466 (2009).
16. F Radicchi, C Castellano, F Cecconi, V Loreto, D Parisi, Defining and identifying communities in networks. *Proc. national academy sciences* **101**, 2658–2663 (2004).
17. M McPherson, L Smith-Lovin, JM Cook, Birds of a feather: Homophily in social networks. *Annu. review sociology* **27**, 415–444 (2001).
18. P Dandekar, A Goel, DT Lee, Biased assimilation, homophily, and the dynamics of polarization. *Proc. Natl. Acad. Sci.* **110**, 5791–5796 (2013).
19. SL Feld, The focused organization of social ties. *Am. journal sociology* **86**, 1015–1035 (1981).
20. DA McFarland, J Moody, D Diehl, JA Smith, RJ Thomas, Network ecology and adolescent social structure. *Am. sociological review* **79**, 1088–1121 (2014).
21. ME Newman, Assortative mixing in networks. *Phys. review letters* **89**, 208701 (2002).
22. ME Newman, J Park, Why social networks are different from other types of networks. *Phys. Rev. E* **68**, 036122 (2003).
23. I Sendiña-Nadal, MM Danziger, Z Wang, S Havlin, S Boccaletti, Assortativity and leadership emerge from anti-preferential attachment in heterogeneous networks. *Sci. reports* **6**, 21297 (2016).
24. D Krackhardt, Structural leverage in marketing in *Networks in marketing*, ed. D Iacobucci. (Sage, Thousand Oaks), pp. 50–59 (1996).
25. A M'Kendrick, Applications of mathematics to medical problems. *Proc. Edinb. Math. Soc.* **44**, 98–130 (1925).
26. F Brauer, The Kermack–McKendrick epidemic model revisited. *Math. biosciences* **198**, 119–131 (2005).
27. HW Hethcote, The mathematics of infectious diseases. *SIAM review* **42**, 599–653 (2000).
28. D Chakrabarti, Y Wang, C Wang, J Leskovec, C Faloutsos, Epidemic thresholds in real networks. *ACM Transactions on Inf. Syst. Secur. (TISSEC)* **10**, 1–26 (2008).
29. BA Prakash, D Chakrabarti, M Faloutsos, N Valler, C Faloutsos, Got the flu (or mumps)? check the eigenvalue! *arXiv preprint arXiv:1004.0060* (2010).
30. D Smith, J Dushoff, R Snow, S Hay, The entomological inoculation rate and plasmodium falciparum infection in african children. *Nature* **438**, 492–495 (2005).
31. MJ Ferrari, et al., The dynamics of measles in sub-saharan africa. *Nature* **451**, 679–684 (2008).
32. M Small, C Tse, Clustering model for transmission of the SARS virus: application to epidemic control and risk assessment. *Phys. A: Stat. Mech. its Appl.* **351**, 499–511 (2005).
33. T Berge, JS Lubuma, G Moremedi, N Morris, R Kondera-Shava, A simple mathematical model for Ebola in africa. *J. biological dynamics* **11**, 42–74 (2017).
34. S Deguen, G Thomas, NP Chau, Estimation of the contact rate in a seasonal SEIR model: application to chickenpox incidence in france. *Stat. medicine* **19**, 1207–1216 (2000).
35. S Riley, et al., Transmission dynamics of the etiological agent of SARS in Hong Kong: impact of public health interventions. *Science* **300**, 1961–1966 (2003).
36. K Prem, et al., The effect of control strategies to reduce social mixing on outcomes of the covid-19 epidemic in Wuhan, China: a modelling study. *The Lancet Public Heal.* (2020).
37. D Caccavo, Chinese and Italian covid-19 outbreaks can be correctly described by a modified sird model. *medRxiv* (2020).
38. B Viswanath, A Mislove, M Cha, KP Gummadi, On the evolution of user interaction in Facebook in *Proc. Workshop on Online Social Networks*. pp. 37–42 (2009).